the assumption made above indeed results in a very small error in this case.

## VI. CONCLUSIONS

The influence of non-ideal integrators on a specified filter transfer function can be analyzed independently of the filter topology using only simple equations in which the quality factor of the integrator is the key parameter. Because the quality factor follows directly from the phase of the integrator as a function of frequency we obtain a practically useful formulation. The example of application demonstrates the possibility to find integrator specifications from the filter specifications. Especially for high frequency continuous-time filters where integrator design is critical it is important to have accurate specifications for the integrator circuits to match.

## APPENDIX A

The modified biquad coefficients in (14):

$$a_2' = \frac{a_2 - a_1 T_2 + a_0 T_2^2}{1 - b_1 T_2 + b_0 T_2^2} \tag{A1}$$

$$a_1' = \frac{\dfrac{2a_2}{T_1} + \left(1 - \dfrac{T_2}{T_1}\right)a_1 - 2T_2 a_0}{1 - b_1 T_2 + b_0 T_2^2} \tag{A2}$$

$$a_0' = \frac{\dfrac{a_2}{T_1^2} + \dfrac{a_1}{T_1} + a_0}{1 - b_1 T_2 + b_0 T_2^2} \tag{A3}$$

$$b_1' = \frac{\dfrac{2}{T_1} + \left(1 - \dfrac{T_2}{T_1}\right)b_1 - 2T_2 b_0}{1 - b_1 T_2 + b_0 T_2^2} \tag{A4}$$

$$b_0' = \frac{\dfrac{1}{T_1^2} + \dfrac{b_1}{T_1} + b_0}{1 - b_1 T_2 + b_0 T_2^2}. \tag{A5}$$

*Case of a First-Order Section:*
With $S = s/\omega_0$ we write for a first-order section:

$$H(S) = \frac{a_1 S + a_0}{S + b_0}. \tag{A6}$$

Replacing $H_{id}(S)$ by $H_{ni}(S)$ from (12) we obtain

$$H'(S) = \frac{a_1' S + a_0'}{S + b_0'}. \tag{A7}$$

Using the same conventions as for the biquad case we find

$$a_1' = \frac{a_1 - a_0 T_2}{1 - b_0 T_2}; \qquad a_0' = \frac{a_0 + \dfrac{a_1}{T_1}}{1 - b_0 T_2}; \qquad b_0' = \frac{b_0 + \dfrac{1}{T_1}}{1 - b_0 T_2}. \tag{A8}$$

For $T_1 \gg 1$ and $T_2 \ll 1$ we find small sensitivities of pole and zero frequencies and dc-gain with respect to $T_1$ and $T_2$.

## REFERENCES

[1] C. F. Chiou and R. Schaumann, "Design and performance of a fully integrated bipolar 10.7 MHz analog bandpass filter," *IEEE J. Solid-State Circuits*, vol. SC-21, pp. 6–14, Feb. 1986.

[2] A. P. Nedungadi and R. L. Geiger, "High frequency voltage-controlled continuous-time lowpass filter using linearised CMOS integrators," *Electron. Lett.*, vol. 22, pp. 729–731, July 1986.

[3] H. Khorramabadi and P. R. Gray, "High frequency CMOS continuous-time filters," *IEEE J. Solid-State Circuits*, vol. SC-19, pp. 939–948, Dec. 1984.

[4] J. M. Khoury and Y. P. Tsividis, "Analysis and compensation of high-frequency effects in integrated MOSFET-C continuous-time filters," *IEEE Trans. Circuits Syst.*, vol. CAS-34, pp. 862–875, Aug. 1987.

[5] K. W. Moulding, J. R. Quartly, P. J. Rankin, and R. S. Thompson, "Gyrator video IC with automatic tuning," *IEEE J. Solid-State Circuits*, vol. SC-15, pp. 963–967, Dec. 1980.

[6] F. Krummenacher and N. Joehl, "A 4-MHz CMOS continuous-time filter with on-chip automatic tuning," *IEEE J. Solid-State Circuits*, vol. 23, pp. 750–758, June 1988.

[7] C. S. Park and R. Schaumann, "Design of a 4-MHz analog integrated CMOS transconductance-C bandpass filter," *IEEE J. Solid-State Circuits*, vol. 23, pp. 987–996, Aug. 1988.

[8] H. Hagiwara, M. Kumazawa, S. Takagi, M. Furihata, M. Nagata, and T. Yanasigawa, "A monolithic video frequency filter using NIC-based gyrators," *IEEE J. Solid-State Circuits*, vol. 23, pp. 172–182, Feb. 1988.

[9] M. S. Ghausi and K. R. Laker, *Modern Filter Design*. Englewood Cliffs, NJ: Prentice-Hall, 1981.

[10] J. R. Brand and R. Schaumann, "Active R filters: Review of theory and practice," *IEE J. Electron. Circuits and Systems*, vol. 2, pp. 89–101, July 1978.

[11] A. S. Sedra and P. Brackett, *Filter Theory and Design: Active and Passive*. Beaverton, OR: Matrix, 1978.

## High-Frequency and High-$Q$ Tunable Active Filters

### YANNICK DEVILLE

*Abstract* — An investigation of the performance of classical second-order bandpass active filters shows that since they use low-gain elements, they can be divided into two classes at high frequencies: low-selectivity stable filters and low-stability selective filters. This paper presents structures that realize a good compromise between both classes, so that high $Q$ can be achieved with good stability. Verifications have been carried out with experimental Si hybrid high-frequency filters and with computer simulations of GaAs microwave integrated filters. The center frequency of the GaAs filters is tuned with MESFET's used as voltage-controlled resistors and can exceed 2 GHz.

## I. INTRODUCTION

At low frequencies, continuous-time active filters can combine high selectivity and stability by using very high-gain operational amplifiers (op amps). However, the gain of high-frequency and microwave amplifiers is limited by stability considerations that are developed hereafter. We will show that second-order bandpass filters using finite-gain amplifiers, which are our main concern here, can be divided into two classes, according to their quality factor $Q$ defined as the ratio of the center frequency to the 3-dB bandwidth:

1) *Class A*: filters that are stable ($Q > 0$) whatever their element values are, but that achieve low selectivity when the use limited values for the voltage gain $K$:

$$Q_{max} = \frac{1}{2} \cdot \sqrt{K + 1}. \tag{1}$$

2) *Class B*: filters that can be selective though using low voltage gain amplifiers:

$$Q = \frac{\alpha}{\beta - K} \tag{2}$$

$\alpha$ and $\beta$ being defined by the passive elements in most cases. As it will be seen $\alpha$ is relatively low, especially in integrated circuits, so that $K$ must be very close to $\beta$ to achieve a high $Q$. The value of $Q$ is then very sensitive to the tolerance of the element parameters and there is a risk of oscillation of the filter ($Q < 0$).

In this paper, we propose a structure based on low-gain elements, which combines high-$Q$ capability and better stability than class B filters, and thus realizes a good compromise between class A and class B. The microwave integrated filters considered here use lumped elements, since their maximum resonant frequency is about 2 GHz.

In the short review of classical filters that follows we will use the terms "class A" and "class B" rather than "negative feedback" and "positive feedback" as they do not relate exactly to one another: the filter contains a loop; the loop phase at the center frequency of the filter $f_p$ verifies $|\varphi_p| \leqslant 180°$. The terms "negative feedback" and "positive feedback" can be interpreted as $|\varphi_p| \geqslant 90°$ and $|\varphi_p| \leqslant 90°$, respectively, while, as can be verified on the following structures, class A and class B, respectively, correspond to

$$\varphi_p \neq 0 \tag{3}$$

and

$$\varphi_p = 0. \tag{4}$$

## II. CLASSICAL LOW-FREQUENCY STRUCTURES

To have a better understanding of the problems that conventional second-order filters face at high frequencies, we will first review the properties that are used at low frequencies in some of the most conventional types.

### 2.1. Filters Based on Medium-Gain Amplifiers

The structures proposed by Sallen and Key in 1955 [1] are among the first low-frequency active filters that were studied. Fig. 1 shows bandpass fiters of that family. The low-pass filters have similar characteristics.

The expression of their selectivity $Q$ shows that they all belong to one of the two classes previously defined (the $Q$ factor of the circuit of Fig. 1(d) with $G > 0$ is slightly different but the problems of sensitivity are exactly the same as with class B filters). Besides, the eighteen circuits proposed by Sallen and Key belong to these classes. It can be verified that class A and class B correspond to (3) and (4) as was mentioned above. For example, the open loop corresponding to the circuit of Fig. 1(a), which is in class A, is given in Fig. 2. $R1$, $C1$, $R2$, and $C2$ realize a high-pass filter whose phase verifies $0 < \psi(f) < 180°$, so that $\varphi_p = \psi(f_p) - 180° \neq 0$.

### 2.2. Filters Based on Op Amps

The emergence of quasi-infinite-gain op amps in the 1960's has made it possible to combine stability and selectivity.

*Finite-Gain Amplifiers using Op Amps*

Low-sensitivity filters have been derived from Class B Sallen and Key filters by two means. 1) Large feedback on op amps has led to voltage amplifiers with a finite gain $K$ entirely defined by



$$Q = \frac{\sqrt{R_1 C_1 R_2 C_2}}{R_1 C_1 + R_1 C_2 + R_2 C_2} \cdot \sqrt{k+1}$$

$$Q_{max} = \frac{1}{2} \sqrt{k+1}$$

$$Q = \frac{\sqrt{R_1 C_1 R_2 C_2} \cdot \sqrt{\frac{R_1}{R_3}+1}}{(R_1 C_1 + R_1 C_2 + R_2 C_2) + \frac{R_1}{R_3} R_2 C_2 (1-k)}$$

$$Q \to \infty \text{ if } k \to k_{max} = 1 + \frac{R_3}{R_1} \cdot \frac{R_1 C_1 + R_1 C_2 + R_2 C_2}{R_2 C_2}$$

$$Q = \frac{\sqrt{R_1 R_2 C_2 [C_1 + C_3 (k+1)]}}{R_1 C_1 + R_1 C_2 + R_2 C_2 + R_1 C_3}$$

$$Q_{max} = \frac{1}{2} \sqrt{k+1}$$

2 possibilities:

$$* \, G > 0 \quad G = k \quad Q = \frac{\sqrt{R_1 C_1 R_2 C_2}}{R_1 (C_1 + C_2) - R_2 C_1 \cdot \frac{1}{k-1}}$$

$$Q \to \infty \text{ if } k \to k_{min} = 1 + \frac{R_2 C_1}{R_1 (C_1 + C_2)}$$

$$* \, G < 0 \quad G = -k \quad Q = \frac{\sqrt{R_1 C_1 R_2 C_2}}{R_1 (C_1 + C_2) + R_2 C_2 \frac{1}{1+k}}$$

$$Q_{max} = \frac{1}{2} \sqrt{k+1}$$
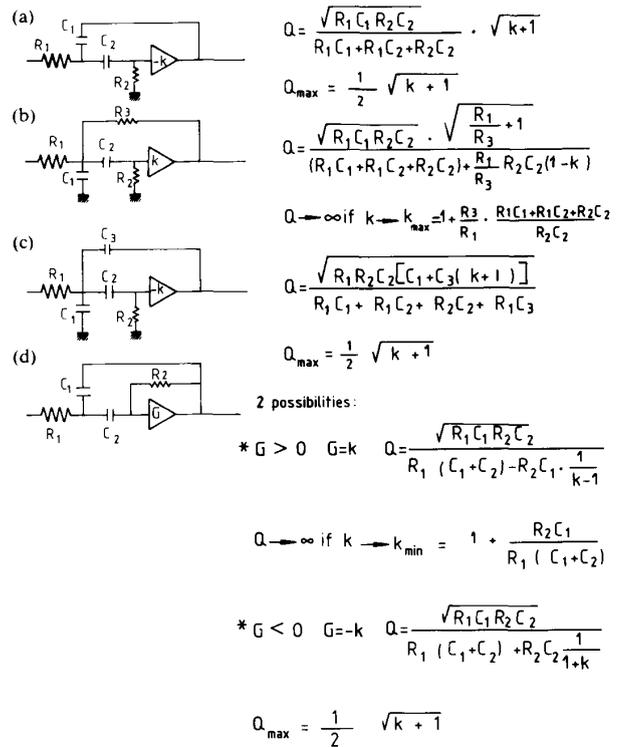
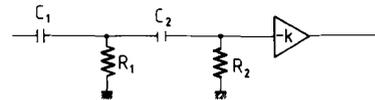Fig. 1.   Sallen and Key bandpass filters.
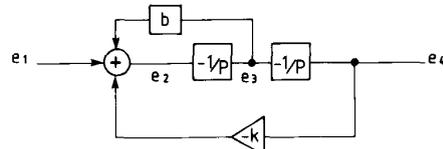


Fig. 2.   Open loop of the circuit in Fig. 1(a).



Fig. 3.   Block diagram of the biquad.

passive elements and thus stable and easy to adjust. For example, the filter of Deliyannis [2] corresponds to the circuit of Fig. 1(d) with $G > 0$ and 2) The $Q$ factor of class B Sallen and Key filters can be expressed as

$$Q = \frac{\alpha}{1 + \gamma - K}. \tag{5}$$

Hence, an op amp with total feedback can be used advantageously: it provides a gain $K$ which is slightly lower than unity, so the filter is stable and its response is only defined by passive elements. However, a high $Q$ is obtained only if the ratios of the passive elements are very large so this solution does not apply to high-$Q$ integrated filters.
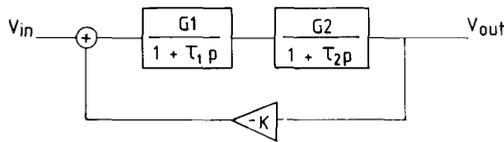
Fig. 4. Biqaud at high frequencies.

*Two-Integrator-Loop Biquads*

Active filters with lossless integrators using op amps have also been realized [3]–[6]. A general block diagram of these filters is shown in Fig. 3. The corresponding $Q$ is given by

$$Q = \frac{\sqrt{K}}{b}. \tag{6}$$

$K$ and $b$ are defined by products of ratios of passive elements. So the filter is always stable, $Q$ is precisely controlled and can be high.

### III. PERFORMANCES OF CLASSICAL STRUCTURES AT HIGH FREQUENCIES

All the filters that have medium or high-$Q$ capabilities contain a loop, with an amplifier made up of stages that can be in different parts of the block diagram. This amplifier creates a phase delay at frequencies close to its cutoff frequency. If this delay causes the loop-phase to be zero at a frequency where the loop-gain is still higher than unity, the filter will oscillate. The first solution to that problem is high-frequency compensation: the transfer function of the loop is modified at high frequencies to ensure stability, either by shifting down the cutoff frequency of one amplifying stage or by inserting a compensation network in the loop. This results in a reduction of the cutoff frequency of the amplifier that can only be accepted if it remains much higher than the center frequency $f_p$ of the filter. This method is thus used in low-frequency filters but is not convenient for high-frequency applications because the cutoff frequency of the un-compensated amplifier is already very close to $f_p$.

Therefore, the only way to ensure the stability of these filters is to lower the overall gain of the loop by reducing the number of amplifying stages (which decreases the phase delay of the amplifier and even more stabilizes the loop). Consequently, the op amps of the low-frequency filters are replaced by finite, and relatively low gain amplifiers, and the circuits become class A and class B filters as will now be shown. This result is obvious for the filters derived from those of Sallen and Key. In the two-integrator-loop biquads, only lossy integrators can be realized (Fig. 4), which results in

$$Q = \frac{\sqrt{\tau_1 \tau_2}}{\tau_1 + \tau_2} \cdot \sqrt{K_{l+1}}, \quad \text{where } K_l = KG_1 G_2 \tag{7}$$

is the loop gain. The filter is a class A filter:

$$Q_{\max} = \frac{1}{2} \cdot \sqrt{K_{l+1}}. \tag{8}$$

So, as previously stated, the most common second-order filters belong to classes A or B at high frequencies. To give an idea of their limitations, the selectivity of class A microwave filters is lower than 2 when the gain of the single-stage amplifier that they use to ensure stability is lower than 10. As for class B filter, if we consider the typical example of the circuit of Fig. 1(b) with $R1 = R2 = R3$ and $C1 = C2$, $K \simeq 4$ is used to obtain a high $Q$
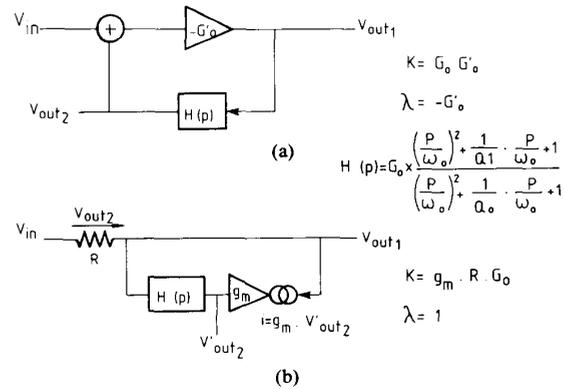


Fig. 5. Block diagrams of the proposed structures.

and the sensitivity of $Q$ to $K$ is very high:

$$S_K^Q = \frac{\partial Q}{\partial K} \cdot \frac{K}{Q} = \frac{K \cdot Q}{\sqrt{2}} \quad (\simeq 140 \text{ if } Q = 50). \tag{9}$$

As for other classical structures, it can be shown that high-frequency Tarmy–Ghausi filters such as in [7] belong to class B, though low-frequency filters of that type [8]–[10] can combine high selectivity and low sensitivity by using all-pass cells based on op amps [11]. Besides, it should be pointed out, that Twin-T feedback filters do not belong to any of classes A and B. They could be regarded as a "class C" but, as they are a special case of the more general structure that is presented in the next section, their characteristics are detailed hereafter.

### IV. PROPOSED STRUCTURES

When a low $K$ is used, it seems that only structures whose $Q$ factor has a denominator of the type $\beta - K$ can provide high $Q$. Those filters require a tuning of $K$ to ensure stability and determine $Q$. However, if the numerator $\alpha$ of $Q$ can be made much larger than with conventional class B filters, the same $Q$ is obtained with $\beta - K$ much larger so that the filter is much less sensitive to $K$ and the $Q$-tuning is easier. The structures that are proposed hereafter are based on these considerations.

#### 4.1. Transfer Functions of the Proposed Structures

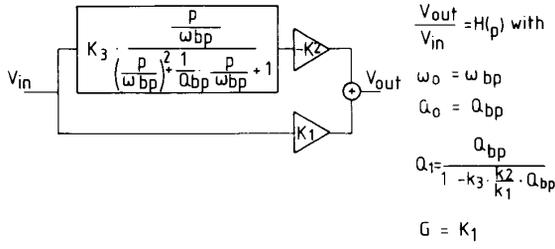Fig. 5 shows two block diagrams that realize the following transfer functions:

$$F(p) = \frac{V_{\text{out1}}}{V_{\text{in}}} = \frac{\lambda}{K+1} \cdot \frac{\left(\dfrac{p}{\omega_p}\right)^2 + \dfrac{1}{Q_0} \cdot \dfrac{p}{\omega_p} + 1}{\left(\dfrac{p}{\omega_p}\right)^2 + \dfrac{1}{Q} \cdot \dfrac{p}{\omega_p} + 1} \tag{10}$$

$$G(p) = \frac{V_{\text{out2}}}{V_{\text{in}}} = \frac{-K}{K+1} \cdot \frac{\left(\dfrac{p}{\omega_p}\right)^2 + \dfrac{1}{Q_1} \cdot \dfrac{p}{\omega_p} + 1}{\left(\dfrac{p}{\omega_p}\right)^2 + \dfrac{1}{Q} \cdot \dfrac{p}{\omega_p} + 1} \tag{11}$$
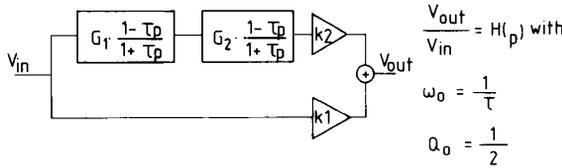
with

$$\omega_p = \omega_0 \tag{12}$$

$$Q = \frac{Q_0(K+1)}{1 + KQ_0/Q_1}. \tag{13}$$

$$\frac{V_{out}}{V_{in}} = H(p) \text{ with}$$

$$\omega_0 = \omega_{bp}$$

$$Q_0 = Q_{bp}$$

$$Q_1 = \frac{Q_{bp}}{1 - k_3 \cdot \frac{k_2}{k_1} \cdot Q_{bp}}$$

$$G = K_1$$



$$\frac{V_{out}}{V_{in}} = H(p) \text{ with}$$

$$\omega_0 = \frac{1}{\tau}$$

$$Q_0 = \frac{1}{2}$$

$$Q_1 = \frac{1}{2} \frac{\sqrt{k_1 + k_2 G_1 G_2}}{k_1 - k_2 G_1 G_2}$$

$$G = k_1 + k_2 G_1 G_2$$

Fig. 6. Cells realizing $H(p)$.

The second circuit provides an additional transfer function, similar to $G(p)$ but with lower gain:

$$G'(p) = \frac{V'_{out2}}{V_{in}} = -\frac{1}{G'_0} G(p). \tag{14}$$

It should be noted that $f_p$ and $Q$ are independent. As $Q_0$ is fixed and much lower than $Q$, $F(p)$ is of the bandpass type. $Q_1$ is a tunable parameter; if $G(p)$ and $G'(p)$ are used $Q_1$ must be quite different than $Q$, otherwise $Q$ does not define the 3-dB bandwidth of these two transfer functions. $G(p)$ and $G'(p)$ realize bandpass responses if $|Q_1|$ is much lower than $Q$ and bandstop responses if it is much higher.

The following considerations about $Q$ apply to the three transfer functions. The availability of the parameter $Q_1$ allows the filter to be used in two ways.

1) Designing for stability: if the filter has to be stable $(Q > 0)$ whatever its element values are, a cell realizing $Q_1 > 0$ whatever its element values are will be used. The cell will be simple, so that the whole filter remains simple. Such cells can achieve

$$Q_0 \approx 1/2. \tag{15}$$

Then, if high $Q_1$ can be obtained:

$$Q \approx 1/2(K+1). \tag{16}$$

The filter is as stable as class A filters but exhibits a much higher $Q$.

2) Designing for selectivity: if $K$ is low, the above value of $Q$ is not high enough. To obtain higher $Q$, a cell realizing a negative $Q_1$ is used. Two possible structures for that cell are given in Fig. 6. For negative $Q_1$, $Q$ can be expressed as

$$Q = \frac{(K+1)|Q_1|}{\frac{|Q_1|}{Q_0} - K}. \tag{17}$$

By using the highest available value of $K$ and consequently choosing $Q_1$, the denominator of (17) is of the type $\beta - K$ as in class B filters but its numerator is much larger. The sensitivity of $Q$ to $K$ is

$$S_K^Q = \left(\frac{Q}{Q_0} - 1\right) \cdot \frac{1}{K+1} \approx \frac{Q}{Q_0} \cdot \frac{1}{K+1} \quad \text{when } Q \text{ is high.}$$

For example, if $Q = 50$ and $Q_0 = 0.5$, $K = 1$; 4; 10; 50, respectively, result in $S_K^Q = 49.5$; 20; 9; 1.9, which should be compared to $S_K^Q = 140$ for class B filters with same selectivity. So, the tuning of an amplifying stage of the proposed structure allows a relatively fine tuning of $Q$. As $Q$ is also tuned by $Q_1$, its sensitivity to the parameter which controls $Q_1$ needs be considered. That sensitivity depends on the structure of the cell $H(p)$. For the first cell of Fig. 6:

$$S_{K3}^{Q} = (Q/Q_0) - 1 \quad (\approx 100 \text{ if } Q = 50 \text{ and } Q_0 = 1/2).$$

For the second cell the expression of $S_{K1}^{Q}$ is more complex and its value is $-28$; $-71$; $-90$; $-103$, respectively for $K = 1$; 4; 10; 50. In both cases, the sensitivities are higher than those to $K$. Therefore, if $K3$ (or $K1$) is realized by an active summer, its tuning has the same accuracy as the tuning of $K$, and $Q$ is more coarsely tuned by $K3$ (or $K1$) than by $K$. However, if $K3$ (or $K1$) is realized by a passive summer, it can be tuned very precisely and it provides a fine tuning of $Q$.

It should be noted that by changing $Q_1$, $H(p)$ can be continuously tuned from a perfect bandstop response ($Q_1$ infinite) to a second-order all-pass response ($Q_1 = -Q_0$). Those two particular cases have been reported in the literature. The bandstop response of the first case has been obtained with a twin-T cell [12], for which $Q_0 = 1/4$. The selectivity of the filter is not high enough for the low $K$ values available in high frequency applications:

$$Q = \frac{1}{4}(K+1). \tag{18}$$

Moreover, infinite $Q_1$ is obtained only for a particular set of values of the elements of the Twin-T, which are tricky to realize. Because of the tuning error, $H(p)$ is of the third order, and uncontrolled effects similar to $Q_1 < 0$ in our structure may appear and result in oscillations of the filter.

The all-pass response of the second case is realized by Tarmy–Ghausi filter, which achieves

$$Q_1 = -Q_0 = -1/2. \tag{19}$$

As $Q_1$ is not free, $K \approx 1$ must be used. Thus this filter cannot take advantage of the use of the highest available $K$.

### 4.2. Experimental Results and Simulations

Practical circuits corresponding to the two proposed structures have been studied. The stages are dc-coupled to avoid low-frequency oscillations. The bandpass characteristic $F(p)$ is considered.

A low-frequency filter (Fig. 7) has first been experimentally tested to verify the validity of our approach. This filter corresponds to the block diagram with a transconductance amplifier and uses the cell $H(p)$ based on all-pass filters. The cell is in the inset of Fig. 7. $P1$ is used to tune $Q1$ and $T1$ is the current source. The experimental results are

- with $Q1$ close to infinity:
  $$f_p = 1176 \text{ Hz}, \quad Q = 260, \quad |F|_{max} = -4.5 \text{ dB}$$

- with $Q1 < 0$:
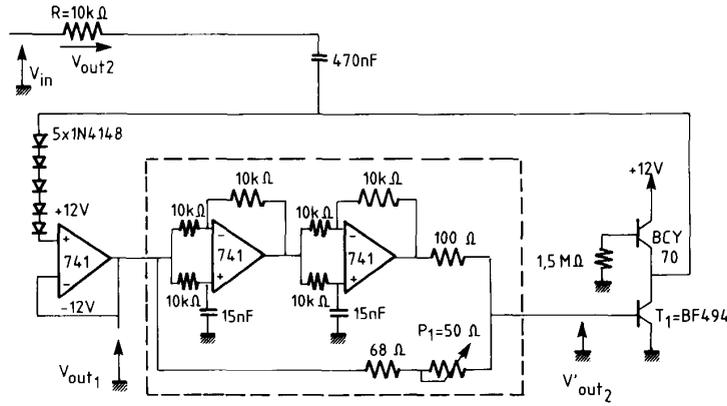  $$f_p = 1176 \text{ Hz}, \quad Q = 950, \quad |F|_{max} = 7.2 \text{ dB}.$$
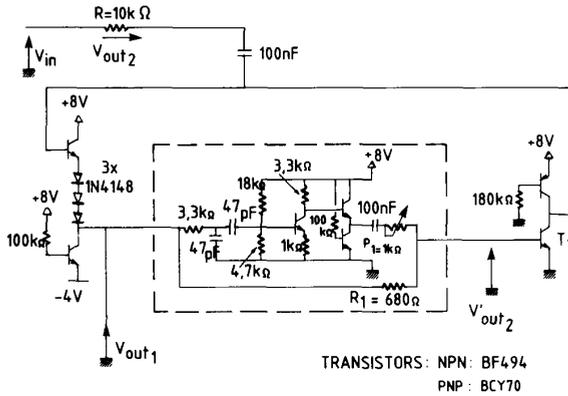
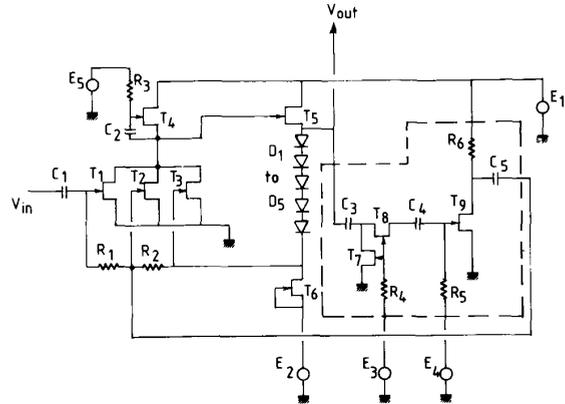Fig. 7.   Low frequency realization.



Fig. 8.   High frequency realization.

TRANSISTORS: NPN: BF494
            PNP : BCY70



Fig. 9.   Microwave realization.

| T1 | 10 μm | R1 | 10 kΩ | E1 | 6 V |
|----|-------|----|-------|----|-----|
| T2 | 35 μm | R2 | 10 kΩ | E2 | -4V |
| T3 | 10 μm | R3 | 10 kΩ | E3 | fp TUNING |
|    |       | R4 | 10 kΩ |    |     |
| T4 | 30 μm | R5 | 20 kΩ | E4 | COARSE Q TUNING |
| T5 | 40 μm | R6 | 600 Ω | E5 | FINE Q TUNING |
| T6 | 25 μm | C1 | 1 pF |  |  |
| T7 | 10 μm | C2 | 1 pF |  |  |
|    |       | C3 | 0.12pF |  |  |
| T8 | 10 μm | C4 | 1 pF |  |  |
| T9 | 40 μm | C5 | 1 pF |  |  |
| D1 to D5 | 25 μm |  |  |  |  |

A high-frequency circuit (Fig. 8) was then experimentally tested. The cell $H(p)$ based on a bandpass filter which is used is in the inset of Fig. 8. Again, $P1$ determines $Q1$, $T1$ is the current source. The following results were obtained.

- $f_p = 664$ kHz, $Q = 53$, $|F|_{max} = -13$ dB
- $f_p = 664$ kHz, $Q = 222$, $|F|_{max} = -2$ dB.

Those values of $Q$ were obtained without any unstability problems, which confirms the ability of the filter to combine stability and selectivity. Finally, practical microwave filters corresponding to the two block diagrams have been simulated. The block diagram with a transconductance amplifier (Fig. 5(b)) can have a higher $K$ than the other one by using a high value $R$. But this advantage disappears in the practical circuits, as the parallel resistor of the current source reduces the gain and quality factor of the filter. Therefore, the block diagram with a voltage amplifier is preferred, as it provides similar sensitivities while having higher gain. The filter also uses the cell $H(p)$ based on a low-selectivity bandpass filter which is in the inset of Fig. 9: $T7$ and $T8$ are used as resistors whose values are defined by $E3$ and determine $f_p$, while $E4$ provides a coarse tuning of $Q1$. $T1$ to $T4$ constitute the amplifier and the summer of Fig. 5 and the summer of the cell $H(p)$. Active summers are used as they have higher gain than passive ones. $E5$ provides a fine tuning of $K$. The circuit response has been simulated using a nonlinear analy-

sis CAD program. The results are

- *center frequency:*
  if $E3 = 0$ V, $f_p = 2.32$ GHz,
  if $E3 = -1.8$ V, $f_p = 1.10$ GHz
  $f_p$ is lower than the center frequency of the bandpass filter of the cell $H(p)$ because of the phase delay of the amplifier.
- *selectivity:*
  $Q$ depends on $E4$ and $E5$: If they are too low $Q$ is low, if they are too high the circuit can become unstable. If $E4$ is controlled within $\pm 25$ mV, it guarantees $34 < Q < 105$ with $Q$ typical $= 50$. Then, $E5$ is tuned and values of $Q$ up to about 100 are obtained with a good accuracy (Table I).

TABLE I
SENSITIVITY OF $Q$ TO $E_S$ ( $E_3 = 0$ V; $E_4 = -0.8$ V )

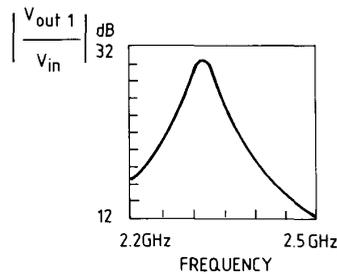| $E_S$ | 2.300 | 2.400 | 2.45 | 2.475 | 2.500 | 2.525 | 2.55 | 2.6 |
|---|---|---|---|---|---|---|---|---|
| $Q$ | 25 | 33 | 40 | 46 | 51 | 61 | 71 | 105 |



Fig. 10. Simulated response.

Naturally, for lower $Q$ applications, the sensitivity of $Q$ to $E5$ decreases. For example, $8.9 < Q < 10.8$ is obtained with $E5$ controlled within $\pm 100$ mV.

As the stages are used close to their cutoff frequency their gain depends on the frequency, so if $f_p$ is changed $E4$ must be changed to obtain the same value of $Q$: if $E5 = 2.5$ V,
at $f_p = 2.32$ GHz, $E4 \simeq -0.8$ V,
at $f_p = 1.10$ GHz, $E4 \simeq -1.95$ V is used.

As an example, the transfer function obtained with $E3 = 0$ V, $E = -0.8$ V, $E5 = 2.5$ V is given in Fig. 10.

## IV. CONCLUSION

The low gain of the available high-frequency and microwave amplifiers does not allow active filters to easily combine stability and selectivity. In this paper, a second-order filter which realizes at high frequencies a good tradeoff between the capabilities of classical structures is presented, with experimental verification. The adjustment of the loop-gain of the structures provides a fine tuning of $Q$, even when a high $Q$ is realized using a low loop-gain. Finally, it should also be remembered that the tuning of $Q$ and $f_p$ can become automatic in integrated filters by use of on-chip master–slaves structures than have been reported in the literature [13]–[17].

### REFERENCES

[1] R. P. Sallen and E. L. Key, "A practical method of designing $RC$ active filters," *IRE Trans. Circuit Theory*, vol. CT-2, pp. 74–85, Mar. 1955.
[2] T. Deliyannis, "High-$Q$ factor circuit with reduced sensitivity," *Electron. Lett.*, vol. 4, pp. 577–579, Dec. 1968.
[3] P. R. Geffe, "RC Amplifier resonators for active filters," *IEEE Trans. Circuit Theory*, vol. CT-15, pp. 415–419, Dec. 1968.
[4] W. J. Kerwin, L. P. Huelsman, and R. W. Newcomb, "State-variable synthesis for insensitive integrated circuit transfer functions," *IEEE J. Solid-State Circuits*, vol. SC-2, pp. 87–92, Sept. 1967.
[5] J. Tow, "A step-by-step active-filter design," *IEEE Spectrum*, vol. 6, pp. 64–68, Dec. 1969.
[6] P. R. Geffe, "Toward high stability in active filters," *IEEE Spectrum*, vol. 7, pp. 63–66, May 1970.
[7] D. J. Comer, "High-frequency narrow-band active filters," *IEEE Trans. Circuits Syst.*, vol. CAS-33, pp. 838–840, Aug. 1986.
[8] R. Tarmy and M. S. Ghausi, "Very high-Q insensitive active $RC$ networks," *IEEE Trans. Circuit Theory*, vol. CT-17, pp. 358–366, Aug. 1970.
[9] G. S. Moschytz, "High-Q factor insensitive active $RC$ network, similar to the Tarmy–Ghausi circuit but using single-ended operational amplifiers," *Electron. Lett.*, vol. 8, pp. 458–459, Sept. 1972.
[10] D. J. Comer and J. E. McDermid, "Inductorless bandpass characteristics using all-pass networks," *IEEE Trans. Circuit Theory*, vol. CT-15, pp. 501–503, Dec. 1968.
[11] J. E. B. Ponsonby, "Active all-pass filter using a differential operational amplifier," *Electron. Lett.*, vol. 2, pp. 134–135, Apr. 1966.
[12] J. Das and K. Ramakrishna, "Twin-T feedback filters," *Int. J. Electron.*, vol. 25, pp. 429–447, Nov. 1968.
[13] C. Chiou and R. schaumann, "Design and performance of a fully integrated bipolar 10.7 MHz analog bandpass filter," *IEEE Trans. Circuits Syst.*, vol. CAS-33, pp. 116–124, Feb. 1986.
[14] K. S. Tan and P. R. Gray, "Fully integrated analog filters using bipolar JFET technology," *IEEE J. Solid-State Circuits*, vol. SC-13, pp. 814–821, Dec. 1978.
[15] M. Banu and Y. Tsividis, "An elliptic continuous-time CMOS filter with on-chip automatic tuning," *IEEE J. Solid-State Circuits*, vol. SC-20, pp. 1114–1121, Dec. 1985.
[16] H. Khorramabadi and P. R. Gray, "High-frequency CMOS continuous-time filters," *IEEE J. Solid State Circuits*, vol. SC-19, pp. 939–948, Dec. 1984.
[17] K. W. Moulding, J. R. Quartly, P. J. Rankin, R. S. Thompson and G. A. Wilson, "Gyrator video filter IC with automatic tuning," *IEEE J. Solid-State Circuits*, vol. SC-15, pp. 963–967, Dec. 1980.

# The Devil's Staircase: The Electrical Engineer's Fractal

MICHAEL P. KENNEDY, KENNETH R. KRIEG,
AND LEON O. CHUA

*Abstract* —In this paper, we describe an *experimental technique* for rapidly and accurately measuring the Devil's Staircase structure of frequency lockings in a periodically forced nonlinear oscillator. This technique uses a personal computer, a programmable oscillator, and a frequency counter. We include an analysis of the method, a discussion of its limitations, and experimental results for two simple test circuits.

## I. INTRODUCTION AND MOTIVATION

An unforced nonlinear oscillator such as the classic van der Pol system [1] has a characteristic "natural frequency" of oscillation $f_u$. If one drives this type of oscillator with a periodic signal of frequency higher than $f_u$ and of sufficiently large amplitude, one finds that the oscillator "locks" onto subharmonics of the driving frequency over broad ranges of frequencies. This synchronization phenomenon is exploited in phase-locking systems throughout broadcast and military electronics. The subharmonic locking effect, called "frequency demultiplication," was reported as early as 1927 by van der Pol and van der Mark [2], who drove a neon bulb $RC$ relaxation oscillator with a sinusoidal voltage, and measured the frequency of the current pulses through the bulb.

Plotting the ratio of the driving frequency to the locked frequency of the circuit against the capacitance $C$ (which determines the natural frequency $f_u$), they obtained a staircase structure of lockings, as shown in Fig. 1 (reproduced from [3]). Similar staircase structures have since been observed in the ac-excited